Journal of
Mechanical
Science and
Technology

Journal of Mechanical Science and Technology 21 (2007) 1855~1868

Review - transport phenomena associated with cells incurring diseases

Jung Yul Yoo* and Yong Ku Lee

School of Mechanical and Aerospace Engineering, Seoul National University, Seoul, 151-744, Korea

(Manuscript Received May 7, 2007; Revised July 12, 2007; Accepted July 27, 2007)

Abstract

Circulatory disease is the number two cause of death next to cancer in Korea, while cardiovascular disease alone is the number one cause of death in the US. Among circulatory diseases, the most intriguing feature of atherosclerosis is that it occurs prevalently at the sites where the endothelium cells are deformed by low wall shear stress (WSS), causing damage to the tunica intimae. Thus, it is shown how computational fluid dynamics (CFD) and medical imaging technique (MIT) can contribute to the diagnosis and the treatment of circulatory diseases in such atherosclerosis-prone sites of blood vessels. On the other hand, people have still suffered from many diseases caused by abnormal proliferation of cancerous cells or bacteria. Thus, it is discussed how human tissue cells and bacteria react to their external fluid media and how their motilities can be analyzed quantitatively by using micro-optical technique and microfluidics.

Keywords: Circulatory disease; Wall shear stress; Computational fluid dynamics; Microfluidics; Review

1. Introduction

Circulatory disease signifies a wide-ranging category of all conditions that affect the heart and the blood vessels. In Korea it is the number two cause of death next to cancer, while cardiovascular disease alone is the number one cause of death in the US. Since the diseases associated with blood circulation have something important to do with the characteristics of blood flow, it is highly important to understand them for improved diagnosis and treatment of circulatory diseases. The most common form of circulatory diseases occurs as a result of atherosclerosis or hardening of the arteries. When this affects the vessels supplying blood and oxygen to heart muscle, it results in coronary heart disease. Hardening of the arteries that supply the brain can result in a stroke. When the arteries to the legs are affected, it results in peripheral vascular disease. The most intriguing feature of atherosclerosis is that it occurs prevalently at the places where the endothelium cells are deformed by low wall shear stress (WSS), causing damage to the tunica intimae. This was pointed out by fluid mechanics theorists in the 80's, and is now widely accepted and believed in the medical community.

There have been many researches to find the relation between blood flow and disease in macroscale and microscale as well. In the present review to examine the transport phenomena associated with cells incurring diseases, we divide the concerned research into two parts. In the first part, we will consider some causes of blood vessel disease, and discuss CFD and experiments associated with blood flow through various arteries closely related to circulatory diseases. Thus, it is shown how CFD and experimental techniques can contribute to the diagnosis and the treatment of circulatory diseases in such atherosclerosis-prone arteries. Then, in the

*Corresponding author. Tel.: +82 2 880 7112, Fax.: +82 2 883 0179
E-mail address: jyyoo@snu.ac.kr

second part, we will review the research on the methods and tools for observing the cell viability and motility from the viewpoint of transport phenomena. It is discussed how human tissue cells and bacteria react to their external fluid media and how their motilities can be analyzed quantitatively. An introduction to a recent visualization study adopting total internal reflection fluorescence (TIRF) and particle tracking velocimetry (PTV) techniques is given, which describes the motion of a single cell in a very shallow region between cell contacts and substrate, say within only several tens of nanometers. In addition, a single-cell chemotaxis experiment is depicted to study the variation of its motility along the gradient of the chemoattractant inside microchannels fabricated by MEMS technique.

2. Circulatory disease caused by deformed endothelial cell

2.1 Causes of circulatory disorder

Circulatory disorders are caused by irregular circulation or blood flow, so it is important to understand the characteristics of the blood and its circulation to diagnose and treat them. Since the time of Virchow (1821-1902), many hemodynamics studies have been carried out to find the causes of the cardiovascular disease [1]. Consequently, it is now widely known that the atherosclerosis is formed near the bifurcation arteries, branch points, and on the region of curvature (see Fig. 1) [2]. These localized formations are also generally accepted to be the result of specific WSS characteristics, especially low WSS [3], high oscillatory shear index (OSI) [4, 5], temporal variation of the shear stress [6], and spatial WSS gradient [7, 8] near those blood vessels.

Vascular endothelial cells (ECs) are constantly exposed to the fluid-mechanical forces generated by flowing blood. ECs are generally aligned in the flow direction and normally deformed. However, locally generated low shear stress deforms the ECs, so that tunica intimae are exposed to the flowing blood, which leads to damages of the tunica intimae. Since Caro et al. [9] postulated that atherosclerotic lesions occur in regions of low WSS as a result of low mass diffusion of lipid, a strong correlation between hemodynamically low WSS and deformation of ECs, leading to atherosclerosis, has been proven by a number of studies [10-13]. Nerem et al. [13] carried out a quantitative study on the shape of ECs from

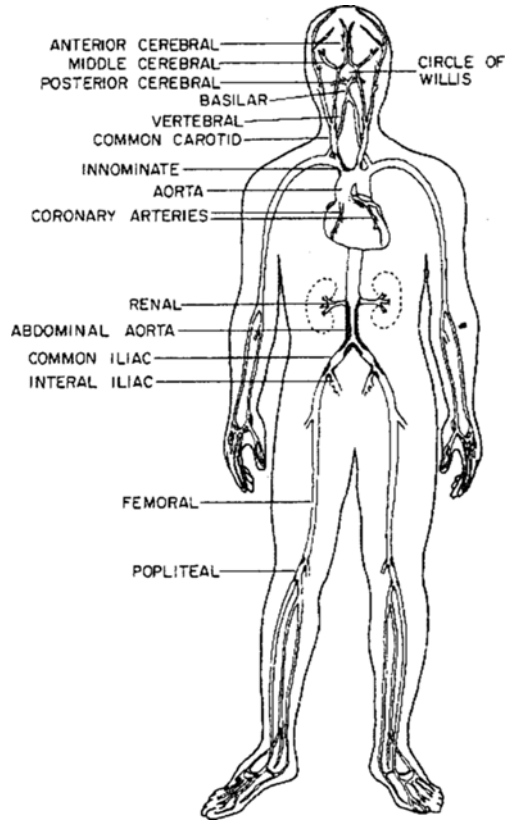

Fig. 1. Pattern of atherosclerosis in humans, showing a concentration of disease in the large and medium-sized arteries [2].

aortic intercostal ostia in rabbits and presented that EC morphology may be a natural indicator of the detailed features of blood flow. Malek et al. [12] studied hemodynamic shear stress and its role in atherosclerosis, by reporting that arterial-level shear stress ($> 15 \times 10^{-3}$ N/m^2) induces endothelial quiescence and an atheroprotective gene expression profile, while low shear stress ($< 4 \times 10^{-3}$ N/m^2), which is prevalent at atherosclerosis-prone sites, stimulates an atherogenic phenotype.

2.2 CFD techniques for hemodynamics

In order to understand and quantify blood flow characteristics in human arteries, numerical methods are widely used. Earlier, mathematically simplified and idealized models were developed to compute velocity and pressure fields of blood flow, which are called 'lumped parameter methods.' Pater et al. [14] proposed a model in which pressure, flow rate, viscous properties, inertial properties of blood, and

elastic blood vessel replace voltage, current, resistors, inductors, and capacitors, respectively. Although lumped parameter methods are useful to provide baseline conditions for other analyses, there are two limitations. First, wave propagation effects are not considered. Second, this model cannot be used to predict the significant spatial distribution of blood flow [15].

Computational methods can be used to realize the wall movement, mass transport, and complexity of geometry. Perktold et al. [16] applied finite element (FE) computer simulation to analyze the pulsatile flow field and the mechanical stresses in a three-dimensional (3D) carotid artery bifurcation model approximated as a rigid wall. To investigate the effect of the distensible artery wall on the local flow field and to determine the mechanical stresses in the artery wall, Perktold and Rappitsch [17] developed a numerical model for the blood flow in the human carotid artery bifurcation. In this model, they incorporated the time-dependent, 3D, incompressible Navier-Stokes equations for non-Newtonian fluids. Giordana et al. [18] considered the effect of geometrical configuration on the steady flow field of representative geometries from an *in vivo* anatomical data set of end-to-side distal anastomoses constructed as part of a peripheral bypass graft. They used a geometrical classification to select the anastomoses of three representative patients according to the angle between the graft and proximal host vessels and the planarity of the anastomotic configuration.

For computational simulation technique, the finite element method (FEM) is generally used because of its excellent applicability to complex geometries. The tissues constituting the blood vessel and human circulatory system have elasticity and are deformed by the force exerted on the tissues. Therefore, to implicate the wall distensibility and model the moving geometries, fluid-structure interaction (FSI) must be considered in conjunction with FEM. As fluid motion is described in Eulerian coordinates while structural motion is described in Lagrangian coordinates, arbitrary Lagrangian-Eulerian (ALE) technique and immersed boundary method (IBM) are generally used [19].

In ALE method, fluid equations are formulated by using ALE coordinates, which are set to be identical to the structural Lagrangian coordinates. Therefore, the computational grid should be updated by using, for example, the elasticity-based mesh-control method proposed by Johnson and Tezduyar [20]. Zhang and Hisada [21] developed a 3D FEM based on ALE technique with structural buckling and large domain changes, and showed its capability by applying it to a two-dimensional (2D) artificial heart simulation and a simplified 3D model with structural buckling and large domain changes. To quantify fluid shear stress and mechanical wall stress, which are difficult to measure *in vivo*, in normal subjects in a clinical setting, and to define regions of low WSS and high mechanical stress, Zhao et al. [22] used a CFD and solid mechanics model with magnetic resonance angiography (MRA), and found significant inter-subject variations in patterns as well as magnitudes of WSS and mechanical stress.

Another method of fluid-structure coupling is the IBM developed by Peskin [23]. The advantage of the IBM is that the entire simulation can be performed on a Cartesian coordinate system without mesh update algorithm. Peskin and McQueen [24] solved the Navier-Stokes equations in the presence of moving immersed boundaries which represent the muscular heart wall and interact with the fluid, by using IBM. Lemmon and Yoganathan [25] also developed a computational model which accounts for blood-tissue interaction under physiological flow conditions and applied it to a thin-walled model of the left heart. Recently, IBM has been further developed in conjunction with adaptive mesh refinement [26] and FEM [27, 28]. In the proposed immersed finite element method (IFEM), the background fluid mesh does not have to follow the motion of the flexible fluid-structure interfaces, so that it is possible to assign a sufficiently refined fluid mesh within the region around the immersed, moving, deformable structures. Using IFEM, Gay et al. [29] studied the mechanical behaviors of angioplasty stents during and after implantation, in terms of FSI. The IFEM is also applied to the modeling of biological systems. Liu et al. [30] modeled the human blood circulation systems using the IFEM, and studied a heart modeling, angioplasty stent development, monocyte and platelet deposition, and red blood cell (RBC) aggregation problems.

Because of the complexity of geometries, FEM and IBM are most widely used to model the human circulatory system. Comparatively fewer studies used finite volume method [31] or finite difference method [32].

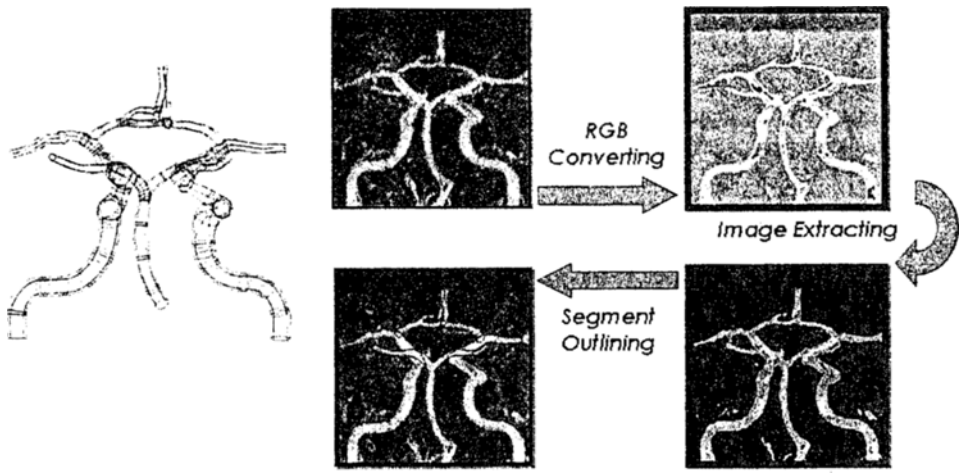

Fig. 2. Image segmentation from MRA for Circle of Willis [33] (permission granted by the ASME International).

2.3 Image-based methods for flows in specific arteries

With the significant advancement in computing power and medical imaging techniques, 3D numerical hemodynamic studies are regarded as providing more realistic tools to treat and diagnose cardiovascular diseases [34]. Recently, for more realistic anatomic geometries, some researchers have begun to introduce the medical imaging data to 3D numerical simulation. These combined techniques have enhanced our understanding of blood flow in the human body, and contributed to the development of medical art for diagnosis and treatment of circulatory disorders. Torii et al. [35] proposed a new numerical FSI technique to investigate the influence of hemodynamic factors in blood vessels from computed tomography (CT) images. Gerbeau et al. [36] proposed strategies for generating the fluid and structure meshes with large displacement and applied them to a congenital cerebral aneurysm coming from medical imaging.

In order to simulate the auto-regulating blood flow in a realistic configuration, an anatomical Circle of Willis (CoW) model was reconstructed from subject-specific MRA images by Kim et al. [33], as shown in Fig. 2. Raw magnetic resonance (MR) images were converted to the RGB graphic file for efficient numerical treatments. After the segments of interest were extracted by filtering the voxels with intensities below a certain threshold, a segment outlining algorithm was used to display the extracted objects on each cross-sectional layer with very little computer memory. A multi-block grid with 32 domains was generated for this geometry. Using this three-dimensionally reconstructed anatomical grid system of about 2 million grid points, simulations of the auto-regulation mechanism of the cerebral arteries were carried out. This numerical model combining CFD and magnetic resonance imaging (MRI) provided the patient-specific information for surgical and interventional procedures as a predictive surgery tool.

Also, since atherosclerosis is mainly generated around the carotid bifurcation arteries, coronary arteries, and abdominal aorta, many researches are carried out on these complex geometries using medical imaging techniques, MRI and CT to reinforce the CFD.

2.4 Carotid arteries

The carotid arteries, which are located on the sides of the neck, supply the brain and face with blood. Because they have a unique carotid sinus or expansion region, atherosclerosis is frequently generated there, which causes the majority of strikes in patients. Ku et al. [37] investigated the spatial and temporal characteristics of blood flow in the normal adult human carotid bifurcation *in vitro* and *in vivo*, by using laser Doppler anemometry (LDA). They suggested that the flow disturbances associated with the normal carotid bifurcation are different from those associated with intraluminal disease and, further, that the secondary flow structures can be usefully employed to establish normalcy. Rindt et al. [38] presented an FE approximation of steady flow in a

rigid 3D model of the carotid artery bifurcation and investigated the influence of the Reynolds number (Re), the flow division ratio, and the bifurcation angle on the axial and the secondary flows in the carotid sinus. However, in these previous studies, simple 3D geometries were used as a computational domain. Thus, it is difficult to give a realistic and quantitative result for treatments. Recently, Cebral et al. [39] developed a noninvasive method for detailed assessment of blood flow patterns and flow rates from directly *in vivo* constructed realistic patient-specific vessel anatomic geometries, which are reconstructed from contrast material-enhanced MRA images with a tubular deformable model, and performed patient-specific CFD modeling based on MR images robustly and efficiently.

2.5 Coronary arteries

To validate the systemic risk factor for atherosclerosis, Friedman et al. [40] suggested that geometric features of atherosclerosis-prone segments can increase the likelihood of disease locally through their influence on the hemodynamic environment of the vessel wall and quantified geometric variables using image processing of multiplane angiograms of the hearts, and morphometry, which was obtained from transverse histologic section at 91 sites. He and Ku [41] performed numerical simulation for the pulsatile hemodynamics of the left coronary artery (LCA) bifurcation using the spectral element method for realistic *in vivo* anatomic and physiologic conditions. The greatest oscillation was localized to the outer wall of the circumflex artery. Bargeron et al. [42] determined the effect of flow partition on wall shear in a cast of a human coronary artery (CA) using a LDA. For pulsatile flow field, Perktold et al. [43] carried out numerical simulation and compared with measured results using Doppler anemometry for the bifurcation of the left anterior coronary artery (LACA) and its first diagonal branch from an anatomically realistic model. Recently, various investigators have reported cellular level studies. Especially, in their studies, RBC's are considered and modeled numerically, so that these results are more realistic and physiologic. Jung et al. [44] performed numerical simulation using the multiphase non-Newtonian theory of dense suspension hemodynamics in a realistic right coronary artery (RCA) having various cross sections. This model predicted higher RBC buildup on the inside radius of curvature. The complex recirculation patterns, the oscillatory flow with flow reversal, and vessel geometry resulted in RBC buildup due to the prolonged particulate residence time, specifically, at the end of the diastole cycle.

2.6 Angiostenosis

Atherosclerosis of the human circulatory system produces major clinical symptoms when the plaque advances to create a high-grade stenosis. Stenoses frequently behave as though the obstruction to flow were variable and not as rigidly fixed. There, pressure lost in flow through a stenosis is the primary determinant of its hemodynamic impact. Brown et al. [45] revealed that three important properties of the stenosis contribute to variation in its pressure loss. First, loss is proportional to the square of stenosis flow. Second, pressure loss is proportional to the inverse fourth power of minimum lumen diameter. Third, a compliant arc of normal arterial wall borders parts of the lumen in the majority of vessel lesions. To quantify the physiologic stress levels experienced by ECs and platelets in the region of vascular stenoses, Siegel et al. [46] solved steady hemodynamic flow field for stenoses with percent area reduction of 50, 75 and 90% over a range of physiologic Reynolds number, Re =100 - 400.

Oshinski et al. [47] evaluated whether MRI and MR phase velocity mapping could provide accurate estimates of stenosis severity and pressure gradient in aortic coarctation. In this study, they introduced a loss coefficient to compare with Doppler ultrasound estimates and suggested that MRI could be used as a complete diagnostic tool for accurate evaluation of aortic coarctation, by determining stenosis location and severity and by accurately estimating pressure gradients. Bluestein et al. [48] analyzed blood flow through a model stenosis with Re = 300 - 3600 using both experimental and numerical methods. According to this study, the jet produced at the throat is turbulent, leading to an axisymmetric region of slowly recirculating flow. For higher Reynolds numbers, this region becomes more disturbed and its length is reduced. Recently, Lorthois et al. [49] calculated the maximum WSS in the convergent part of a stenosis using a dimensional analysis based on the interactive boundary-layer theory.

2.7 Aneurysm

Hashimoto et al. [50] investigated the relationship of hemodynamics in the CoW to the development of cerebral aneurysms by comparing with findings from rats experiments and lesions in man, and proposed that cerebral aneurysms developed on the vessel where hemodynamic stresses were apparently increased. Low et al. [51] examined the flow characteristics in two lateral model aneurysms by means of numerical simulation of governing Navier-Stokes equations describing incompressible, pulsatile, 3D non-Newtonian flow with FEM. This study concentrated on basic flow and stress patterns in a rigid wall and in distensible wall aneurysms. In order to evaluate the shear stress and pressure gradients acting on the aneurysm wall under a variety of flow and geometric conditions, Burleson et al. [52] developed the 2D FE computer model of lateral aneurysms in a steady flow. Lieber et al. [53] examined the influence of stents. In general, it has been known that intravascular stents traversing the orifice may lead to thrombosis and subsequent occlusion of the aneurysm by clinical observations and experimental studies. To validate the experimental and numerical models and to determine the temporal evolution of WSS downstream of the stenosis under the pulsatile flow condition, 2D velocity measurements are performed in a 75%-severity stenosis using a pulsed Doppler ultrasonic velocimeter and transient numerical simulation are carried out by Deplano and Siouffi [54]. The key result of the study is that the presence of the stenosis leads the artery to work in a direction which is opposite to the direction of a healthy artery.

Recently, image-based computational simulations have been widely used to investigate the hemodynamics of aneurysms. Steinman et al. [55] carried out the numerical simulation combined with computed rotational angiography to provide hemodynamic information in a patient-specific manner for a giant intracranial aneurysm. They suggested that since this method is anatomically realistic and patient-specific, such image-based CFD analysis may be used to provide key hemodynamic information for prospective studies of aneurysm growth and rupture or to predict the response of an individual aneurysm to therapeutic options. Stuhne and Steinman [56] adopted mesh convergence technology - conformal meshing technique - to CFD simulation to model the flow characteristics of stented aneurysms. They utilized general-purpose computer-assisted design and unstructured mesh generation tools that apply in principle to stents and vasculature of arbitrary complexity. A mesh convergence analysis for stented steady flow was performed, varying node spacing near the stent. Physiologically pulsatile simulations were then performed using the converged mesh.

2.8 Pulsatile flow

Womersley [57] established one of the most fundamental theories on pulsatile flow characteristics that are essential to realistic hemodynamic studies. Although he ignored the motion of the wall, he presented a theoretical solution for pulsatile flow by linearizing the basically nonlinear equations, which provided the fundamental reference. Since then, numerous studies have been carried out to investigate the effect of the pulsatile flow on the atherosclerosis.

Friedman et al. [58] carried out numerical simulation of pulsatile blood flow through a symmetrical branch modeling the aortic bifurcation to assess hemodynamic theories of atherosclerosis by comparing the distribution of hemodynamic variables with that of early lesions in arterial branch. As a theoretical study, Mehrotra et al. [59] obtained an analytic solution for pulsatile laminar flow in an elliptic tube for stenosis in arteries. Wang and Tarbell [60] performed a numerical analysis to study the effect of the flow at the instance of acceleration and deceleration on the strain-rate on the wall, pressure and velocity distributions by using a perturbation solution. To understand the hemodynamic properties more precisely, Taylor et al. [5] developed a comprehensive computational framework based on a 3D FEM to solve the governing equations for pulsatile flow in the abdominal aorta (AA). They showed that the numerical investigation provides detailed quantitative data on hemodynamic conditions. Zendehbudi and Moayeri [61] presented a numerical solution for physiological pulsatile and equivalent simple pulsatile flows, and discussed the differences in their flow behaviors.

Recently, Zeng et al. [62] investigated the effects of physiologically realistic cardiac-induced motion on hemodynamics in human RCA modeled as fixed and moving vessels, and concluded that the hemodynamic effects of RCA motion can be ignored as an approximation in modeling research. Using com-

mercial code, Varghese and Frankel [63] modeled pulsatile turbulent flow in stenotic vessels based on Reynolds-averaged Navier-Stokes equation and verified the model with two different experimental studies and four different numerical studies with four different turbulent models. MRI technique is also used to investigate the effect of pulsatile flow on the circulatory disease. Marshall et al. [64] studied pulsatile flow in physiologically realistic models of normal and moderately stenosed (30% diameter reduction) human carotid bifurcation. Time-resolved velocity measurements were made by using MRI, from which WSS vectors were calculated.

2.9 Non-Newtonian flow

The rheological behavior of blood can be characterized by a shear-rate-dependent non-Newtonian viscosity and its viscoelasticity. To investigate the effect of the non-Newtonian viscosity of blood on the flow in a coronary arterial casting of man, numerical study using FEM was carried out by Cho and Kensey [65]. In this study, various constitutive models were examined to model the non-Newtonian viscosity of blood and their constants were summarized. Among several constitutive models, Lou and Yang [66] used the Casson equation to describe blood rheology and performed 2D numerical simulation. While Tu and Deville [67] carried out numerical studies for the blood flow through stenoses using the Herschel-Bulkley model, Bingham plastic model and power-law model for steady and pulsatile flows.

In the 1990's, Gijsen et al. [68, 69] performed LDA experiments and FE simulation of steady [69] and unsteady [68] flows in a 3D model for the carotid bifurcation in order to investigate the influence of non-Newtonian blood analog fluid and a Newtonian reference fluid. In these studies, the Carreau-Yasuda model was incorporated. As a result, the axial velocity field of the non-Newtonian fluid was flattened, had lower velocity gradients at the divider wall, and higher velocity gradients at the non-divider wall. And the flow separation, as found with the Newtonian fluid, was absent.

Recently, Rohlf and Tenti [70] clarified the meaning of Womersley number (Wo) in pulsatile blood flow in small vessels using a dimensional analysis based on the Casson model for rheological properties of blood. Johnston et al. [71] carried out numerical simulation of the blood flow through four different RCAs using five non-Newtonian models, as well as the Newtonian model. In this study, local and global non-Newtonian importance factors are introduced, in an attempt to quantify the types of flows where non-Newtonian behavior is significant. Amornsmankul et al. [72] modeled the inner layer of arterial wall as a porous medium and performed numerical study for non-Newtonian blood flow.

3. Cell responses from the biophysical and biochemical viewpoint

3.1 Cell viability and motility

According to the Encyclopedia of Science and Technology [5th edition, McGraw-Hill Co., Inc.], understanding how cells move increases the ability to control abnormal cell behavior, such as the increased level of cell division responsible for cancer and the migration of cancer cells from their site of origin in the body. Errors in chromosome segregation are also known to be responsible for Down syndrome, and are prevalent during the progression of neoplastic tumors. Because the normal functioning of cells is so dependent on proteins that compose and regulate microtubules and actin filaments, defects in these proteins are expected to have severe effects on cell viability. An example of a microtubule defect has been identified in Alzheimer's disease: a microtubule-associated protein is found to be a prominent component of abnormal neurofibrillary tangles seen in affected nerve cells.

Cell viability is also an important factor to determine whether the culturing condition is suitable, particularly in drug screening cases whether the candidate drug is reliable or not. The cell viability can be quantified by measuring cell motility (adhesion and migration). Adherent cell motility plays an essential role in a variety of biological processes; embryonic development, inflammation, tissue repair, angiogenesis, and tumor invasion [73]. Many researches have been carried out about cell-substratum adhesion for observing cell motility more closely, because knowledge of the pattern of contacts between a cell and the surface on which it is spread is essential to the understanding of cell attachment and movement on solid substrate. Smilenov et al. [74] reported 2D motility of focal-adhesion by tracking GFP (green fluorescent protein)-labeled integrin. Regarding non-adherent cells, many attempts have

used bacteria in order to solve problems of microscale hydrodynamics such as mixing enhancement [75] and flow generation [76]. There have been many studies concerning near-surface bacterial motion [77-79].

3.2 EC motility under shear stress condition

Several research groups have examined the biologically important flow behaviors in some detail. Satcher et al. [80] considered the endothelial surface which varies sinusoidally in height, with the wavelength of the variations different in the directions parallel to and normal to the flow, and thus accounted for the elongation seen in ECs subject to steady shear stress. Mammalian cells exhibit a wide range of shear sensitivity with respect to the stress level required to cause overt lysis and death. Some recent evidence suggests that shear stress may have beneficial effects on cellular metabolism and possibly viability at lower levels. Barbee et al. [81] reported the first topographical data of the surface of living ECs at sub-light-microscopic resolution. The measurements were essential to a detailed understanding of force distribution in the endothelium subject to flow. Davies et al. [82] found that the turbulent fluid shear stress induces vascular EC turnover *in vitro*. They suggested that in atherosclerotic lesion-prone regions of the vascular system, unsteady blood flow characteristics, rather than the magnitude of WSS, may be the major determinant of hemodynamically induced EC turnover. Not only the magnitude of shear stress but also its direction could affect the morphological responses of live cells. Frangos et al. [83] developed a flow apparatus for study of the metabolic response of adherent cells to a wide range of steady and pulsatile shear stresses under well-controlled conditions. Human umbilical vein EC monolayers were subject to steady shear stresses and the production of prostacyclin was determined. This study demonstrates that shear stress in certain ranges may not be detrimental to mammalian cell metabolism. In fact, throughout the range of shear stresses studied, metabolite production is maximized by maximizing the shear stress. According to the research of Kataoka et al. [84], ECs could be expected to recognize the flow direction, and change their shape and F-actin structure. After flow exposure, the shape index (SI) and angle of cell orientation were measured, and F-actin distributions in the cells were statistically studied. ECs under the one-way flow condition showed marked elongation and aligned with the flow direction.

Numerical as well as experimental approaches were carried out regarding the motility of live cells

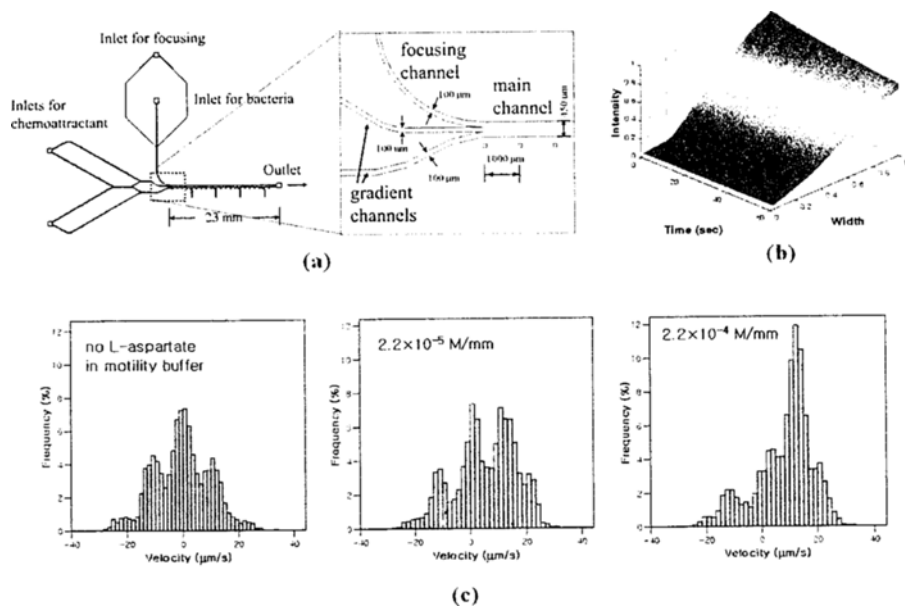

Fig. 3. Quantitative analysis of single bacterial chemotaxis using a hydrodynamic focusing channel [85]. (a) Device for microfluidic chemotaxis assays, (b) Variation of intensity of Rhodamine B with time, (c) Distribution of the velocities measured at intervals of 0.1 s in various concentration gradients of L-aspartate.

exposed to fluid shear stress [81, 86]. A 3D CFD model of ECs simulating cell shape was designed, in order to address questions concerning why and how the morphology of ECs forms under the shear stress loading [86]. A full 3D non-linear CFD simulation was conducted to estimate the WSS distribution. After a finite interval of the flow computation, only the infinitesimal configuration changes that reduced the WSS were allowed to accumulate. As a result of the very long free-run computation experiment, starting with a sub-confluent pattern of cells, the model cells became confluent and were elongated and aligned, with a shape index (SI) very close to that reported for cells *in vivo*.

3.3 Cell motility under chemical stimulation

Chemotaxis is the response of the cells to chemical stimuli. It is one of the most basic and fascinating processes in nature, involved in both health and disease. The knowledge about chemotaxis has been accumulated over the past 40 years. Two general categories can be conveniently made: population and individual cell studies. Because bacterial chemotaxis has a significant impact on the study of structure and function of bacteria, quantification of chemotactic motion is necessary to identify chemoattractant and to determine the bacterial transport parameters used in prediction models of chemotaxis. Mesibov et al. [87] developed a capillary assay for bacterial chemotaxis. This simple approach is most helpful for qualitative comparison of relative responses of bacteria to different chemicals. Ford et al. [77] suggested a device named the stopped–flow diffusion chamber. They measured the chemotaxis as they stopped the flow in this chamber. Recently, microfluidic assays have been developed to generate the concentration gradient of chemoattractants [88-90].

Jeon et al. [89] developed a microfluidic device, as shown in Fig. 3, which measures the velocity of bacteria in response to a concentration gradient of chemoattractant by using particle tracking velocimetry (PTV). A unique feature of this microfluidic device is that after a linear concentration gradient of chemoattractant is generated in the main channel only by diffusion of the chemicals, bacteria are injected into the main channel in single file by a hydrodynamic focusing technique. Then the motility of bacteria in response to various concentration gradients of chemoattractant is measured and analyzed statistically and quantitatively. In this study they obtained a distribution of velocity while bacteria are swimming and tumbling in the presence of the linear concentration gradient of L-aspartate as chemoattractant. By analyzing the distribution, the characteristic motility of the bacteria according as the condition of concentration was obtained. Additionally, the degree of chemotaxis could be quantified by analyzing the distribution of the velocity with the definition of a novel coefficient, Migration Rate, which means how much the cells have chemotaxis.

Lee et al. [91] carried out an image analysis of living cells forming their contacts at the bottom of the cell culturing substrate. In order to visualize the contact area selectively, they adopted the total internal reflection fluorescence (TIRF) method, which can illuminate the cell contact within the adhesion region specifically and detect its fluorescence not being interrupted by other fluorescence from the cell body far from the substrate. From the fluorescence intensity of the TIRF image, they could calculate the distance of the cell surface from the substrate. As a result, they visualized the origin of cell contacts, their movements, and the change of cell-contact type from the close-contact into focal-contact with information of its vertical displacement representing the temporal evolution process of the 3D cell-to-surface profile near the contact area during this metamorphosis. Moreover, they obtained time-series TIRF images which showed that cell contacts were developing or decaying under various conditions: normal and various toxic environments, which can represent various concentration conditions of drug candidates in screening to determine the most appropriate drug composition [92].

Cancer cells possess a broad spectrum of migration and invasion mechanisms. These include both individual and collective cell-migration strategies. Cancer therapeutics for targeting adhesion receptors or proteases have not proven to be effective in slowing tumor progression in clinical trials — this might be due to the fact that cancer cells can modify their migration mechanisms in response to different conditions [93]. However, metastasis of cancer cells is initiated by the cellular migration into extracellular matrix and surrounding vessels. Murata et al. [94] previously showed that elevation of a specific chemical density levels in cancer cells suppressed trans-cellular migration *in vitro*. Drugs that can elevate the levels in cancer cells effectively may be

applied to prevent metastasis in cancer patients. In the trans-cellular migration assay, the presented drug suppressed cancer cell invasion. Thus, it can suppress colon cancer cell motility and might be effective as an anti-metastasis drug for cancer patients.

4. Conclusions

We have reviewed a large number of researches on hemodynamics and cell responses in view of transport phenomena associated with cells incurring diseases. The first part of this review deals with circulatory diseases caused by deformed ECs, and the second part deals with cell responses from the biophysical and biochemical viewpoint.

In part one, we discussed how fluid mechanics has contributed to the identification of the sites where circulatory diseases occur and how the CFD and MIT techniques can contribute to the macroscale diagnosis and treatment of circulatory disorders. More specific examples of hemodynamic studies on atherosclerosis have been given with regard to carotid arteries, coronary arteries, angiostenosis and aneurysms. Further, some efforts that were made to incorporate the pulsatile flow in arteries and the non-Newtonian behavior of the blood in hemodynamic studies have been discussed. In part two, we presented the microscale biophysical and biochemical approaches involving micro technology and cell physiology. In particular, EC motility under shear stress condition and cell motility under chemical condition was discussed.

By integrating new understanding of macroscale and microscale cell fluid mechanics, we could develop more effective diagnostic techniques and novel medical equipments.

Acknowledgments

This work was supported by grant No. R01-2005-000-10558-0 from the Basic Research Program of the Korea Science & Engineering Foundation (KOSEF) and grant No. 2006-017-04 from Korean Small and Medium Business Administration (SMBA). The authors are thankful to Mr. Hyun Woo Lee for his kind assistance in writing this article.

References

[1] M. Bonert, R. L. Leask, J. Butany, C. R. Ethier, J. G. Myers, K. W. Johnston and M. Ojha, The relationship between wall shear stress distributions and intimal thickening in the human abdominal aorta, *Biomed. Eng. Online*. 2 (2003) 18.

[2] D. M. Spain, Atherosclerosis, *Scient. Am.* 215 (1966) 49.

[3] S. S. White, C. K. Zarins, D. P. Giddens, H. Bassiouny, F. Loth, S. A. Jones and S. Glagov, Hemodynamic patterns in two models of end-to-side vascular graft anastomoses: effects of pulsatility, flow division, Reynolds number, and Hood Length, *ASME J. Biomech. Eng.* 115 (1993) 104-111.

[4] C. A. Taylor, M. T. Draney, J. P. Ku, D. Parker, B. N. Steele, K. Wang and C. K. Zarins, Predictive medicine: computational techniques in therapeutic decision-making, *Comput. Aided Surg.* 4 (1999) 231-247.

[5] C. A. Taylor, T. J. R. Hughes and C. K. Zarins, Finite element modeling of three-dimensional pulsatile flow in the abdominal aorta: relevance to atherosclerosis, *Ann. Biomed. Eng.* 26 (1998) 975-987.

[6] M. Ojha, Wall shear stress temporal gradient and anastomotic intimal hyperplasia, *Circ. Res.* 74 (1994) 1227-1231.

[7] C. Kleinstreuer, M. Lei and J. P. Archie Jr., Flow input waveform effects on the temporal and spatial wall shear stress gradients in a femoral graft-artery connector, *ASME J. Biomech. Eng.* 118 (1996) 506-510.

[8] M. Lei, J. P. Archie and C. Kleinstreuer, Computational design of a bypass graft that minimizes wall shear stress gradients in the region of the distal anastomosis, *J. Vasc. Surg.* 25 (1997) 637-646.

[9] C. G. Caro, J. M. Fitz-Gerald and R. C. Schroter, Arterial wall shear and distribution of early atheroma in man, *Nature*. 223 (1969) 1159-1161.

[10] N. DePaola, M. A. Gimbrone Jr., P. F. Davies and C. F. Dewey Jr., Vascular endothelium responds to fluid shear stress gradients, *Arterioscler. Thromb.* 12 (1992) 1254-1257.

[11] C. F. Dewey Jr., S. R. Bussolari, , M. A. Gimbrone Jr. and P. F. Davies, The dynamic response of vascular endothelial cells to fluid shear stress, *ASME J. Biomech. Eng.* 103 (1981) 177-185.

[12] A. M. Malek, S. L. Alper and S. Izumo, Hemodynamic shear stress and its role in atherosclerosis, *JAMA*. 282 (1999) 2035-2042.

[13] R. M. Nerem, M. J. Levesque and J. F. Cornhill, Vascular endothelial morphology as an indicator of the pattern of blood flow, *ASME J. Biomech. Eng.* 103 (1981) 172-176.

[14] L. de Pater and J. W. van den Berg, An electrical analogue of the entire human circulatory system, *Med. Electron. Biol. Engng.* 2 (1964) 161-166.

[15] C. A. Taylor and M. T. Draney, Experimental and Compuational Methods in Cardiovascular Fluid Mechanics, *Annu. Rev. Fluid Mech.* 36 (2004) 197-231.

[16] K. Perktold, R. Peter, M. Resch and G. Langs, Pulsatile non-Newtonian blood flow in three-dimensional carotid bifurcation models: a numerical study of flow phenomena under different bifurcation angles, *J. Biomed. Eng.* 13 (1991) 507-515.

[17] K. Perktold and G. Rappitsch, Computer simulation of local blood flow and vessel mechanics in a compliant carotid artery bifurcation model, *J. Biomech.* 28 (7) (1995) 845-856.

[18] S. Giordana, S. J. Sherwin, J. Peiró, D. J. Doorly, J. S. Crane, K. E. Lee, N. J. W. Cheshire and C. G. Caro, Local and global geometric influence on steady flow in distal anastomoses of peripheral bypass grafts, *ASME J. Biomech. Eng.* 127 (2005) 1087-1098.

[19] T. Yamaguchi, Ishikawa, K. Tsubota, Y. Imai, M. Nakamura and T. Fukui, Computational blood flow analysis - new trends and methods, *J. Biomech. Sci. Eng.* 1 (1) (2006) 29-50.

[20] A. A. Johnson and T. E. Tezduyar, Mesh update strategies in parallel finite element computations of flow problems with moving boundaries and interfaces, *Comput. Methods Appl. Mech. Engrg.* 119 (1994) 73-94.

[21] Q. Zhang and T. Hisada, Analysis of fluid-structure interaction problems with structural buckling and large domain changes by ALE finite element method, *Comput. Methods Appl. Mech. Eng.* 190 (2001) 6341-6357.

[22] S. Z. Zhao, B. Ariff, Q. Long, A. D. Hughes, S. A. Thom, A. V. Stanton and X. Y. Xu, Inter-individual variations in wall shear stress and mechanical stress distributions at the carotid artery bifurcation of healthy humans, *J. Biomech.* 35 (2002) 1367-1377.

[23] C. S. Peskin, Numerical analysis of blood flow in the heart, *J. Comput. Phys.* 25 (1977) 220-252.

[24] C. S. Peskin and D. M. McQueen, A three-dimensional computational method for blood flow in the heart. I. immersed elastic fibers in a viscous incompressible fluid, *J. Comput. Phys.* 81 (1989) 372-405.

[25] J. D. Lemmon and A. P. Yoganathan, Three-dimensional computational model of left heart diastolic function with fluid-structure interaction, *ASME J. Biomech. Eng.* 122 (2000) 109-117.

[26] A. M. Roma, C. S. Peskin and M. J. Berger, An adaptive version of the immersed boundary method, *J. Comput. Phys.* 153 (1999) 509-534.

[27] X. Wang and W. K. Liu, Extended immersed boundary method using FEM and RKPM, *Comput. Methods Appl. Mech. Engrg.* 193 (2004) 1305-1321.

[28] L. Zhang, A. Gerstenberger, X. Wang and W. K. Liu, Immersed Finite Element Method, *Comput. Methods Appl. Mech. Engrg.* 193 (2004) 2051-2067.

[29] M. Gay, L. Zhang and W. K. Liu, Stent modeling using immersed finite element method, *Comput. Methods Appl. Mech. Engrg.* 195 (2006) 4358-4370.

[30] W. K. Liu, Y. Liu, D. Farrell, L. Zhang, X. S. Wang, Y. Fukui, N. Patankar, Y. Zhang, C. Bajaj, J. Lee, J. Hong, X. Chen and H. Hsu, Immersed finite element method and its applications to biological systems, *Comput. Methods Appl. Mech. Engrg.* 195 (2006) 1722-1749.

[31] D. Lee and J. J. Chiu, Intimal thickening under shear in a carotid bifurcation - a numerical study, *J. Biomech.* 29 (1996) 1-11.

[32] D. Tang, C. Yang, S. Kobayashi and D. N. Ku, Generalized finite difference method for 3-D viscous flow in stenotic tubes with large wall deformation and collapse, *Appl. Numer. Math.* 38 (2001) 49-68.

[33] C. S. Kim, C. Kiris, D. Kwak and T. David, Numerical simulation of local blood flows in carotid and cerebral arteries under altered gravity, *ASME J. Biomech. Eng.* 12 (2) (2005) 194-202.

[34] C. A. Taylor, T. J. R. Hughes and C. K. Zarins, Effect of exercise on hemodynamic conditions in the abdominal aorta, *J. Vasc. Surg.* 29 (1999) 1077-1089.

[35] R. Torii, M. Oshima, T. Kobayashi, K. Takagi and T. E. Tezduyar, Fluid-structure interaction modeling of aneurysmal conditions with high and normal blood pressures, *Comput. Mech.* 38 (2006) 482-490.

[36] J.-F. Gerbeau, M. Vidrascu and P. Frey, Fluid-structure interaction in blood flows on geometries based on medical imaging, *Computers and Structures*, 83, (2005) 155-165.

[37] D. N. Ku, D. P. Giddens, D. J. Phillips and D. E. Strandness Jr., Hemodynamics of the normal human bifurcations: in vitro and in vivo studies, *Ultrasound Med. Biol.* 11 (1985) 13-26.

[38] C. C. Rindt, A. A. van Steenhoven, J. D. Janssen, R. S. Reneman and A. Segal, A numerical analysis of steady flow in a three-dimensional model of the carotid artery Bifurcation, *J. Biomech.* 23 (1990) 461-473.

[39] J. R. Cebral, P. J. Yim, R. Löhner, O. Soto and P. L. Choyke, Blood flow modeling in carotid arteries with computational fluid dynamics and MR Imaging, *Acad. Radiol.* 9 (2002) 1286-1299.

[40] M. H. Friedman, P. B. Baker, Z. Ding, and B. D. Kuban, Relationship between the geometry and quantitative morphology of the left anterior descending coronary artery, *Atherosclerosis*, 125 (1996) 183-192.

[41] X. He and D. N. Ku, Pulsatile flow in the human left coronary artery bifurcation: average conditions, *ASME J. Biomech. Eng.* 118 (1996) 74-82.

[42] C. B. Bargeron, O. J. Deters, F. F. Mark and M. H. Friedman, Effect of flow partition on wall shear in a cast of a human coronary artery, *Cardiovasc. Res.* 22 (1988) 340-344.

[43] K. Perktold, M. Hofer, G. Rappitsch, M. Loew, B. D. Kuban and M. H. Friedman, , "Validated Computation of Physiological Flow in a Realistic Coronary Artery Branch," *J. Biomech.*, Vol. 31 (1998) 217-228.

[44] J. Jung, R. W. Lyczkowski, C. B. Panchal and A. Hassanein, Multiphase hemodynamic simulation of pulsatile flow in a coronary artery, *J. Biomech.* 39 (2006) 2064-2073.

[45] B. G. Brown, E. L. Bolson and H. T. Dodge, Dynamic mechanisms in human coronary stenosis, *Circulation.* 70 (1984) 917-922.

[46] J. M. Siegel, C. P. Markou, D. N. Ku and S. R. Hanson, A scaling law for wall shear rate through an arterial stenosis, *ASME J. Biomech. Eng.* 116 (1994) 446-451.

[47] J. N. Oshinski, W. J. Parks, C. P. Markou, H. L. Bergman, B. E. Larson, D. N. Ku, S. Mukundan Jr. and R. I. Pettigrew, Improved measurement of pressure gradients in aortic coarctation by magnetic resonance imaging, *J. Am. Coll. Cardiol.* 28 (1996) 1818-1826.

[48] D. Bluestein, L. Niu, R. T. Schoephoerster and M. K. Dewanjee, Fluid mechanics of arterial stenosis: relationship to the development of mural thrombus, *Ann. Biomed. Eng.* 25 (1997) 344-356.

[49] S. Lorthois, P.-Y. Lagrée, J.-P. M. Vergnes and F. Cassot, Maximal wall shear stress in arterial stenoses: application to the internal carotid arteries, *ASME J. Biomech. Eng.* 122 (2000) 661-666.

[50] N. Hashimoto, H. Handa, I.. Nagata and F. Hazama, Experimentally induced cerebral aneurysms in rats: part V. relation of hemodynamics in the circle of willis to formation of aneurysms, *Surg. Neurol.* 13 (1980) 41-45.

[51] M. Low, K. Perktold and R. Raunig, Hemodynamics in rigid and distensible saccular aneurysms: a numerical study of pulsatile flow characteristics, *Biorheology.* 30 (1993) 287-298.

[52] A. C. Burleson, C. M. Strother and V. T. Turitto, Computer modeling of intracranial saccular and lateral aneurysms for the study of their hemodynamics, *Neurosurgery.* 41 (1997) 326-327.

[53] B. B. Lieber, A. P. Stancampiano and A. K. Wakhloo, Alteration of hemodynamics in aneurysm models by stenting: influence of stent porosity, *Ann. Biomed. Eng.* 25 (1997) 460-469.

[54] V. Deplano and M. Siouffi, Experimental and numerical study of pulsatile flows through stenosis: wall shear stress analysis, *J. Biomech.* 32 (1999) 1081-1090.

[55] D. A. Steinman, J. S. Milner, C. J. Norley, S. P. Lownie and D. W. Holdsworth, Image-Based Computational Simulation of Flow Dynamics in a Giant Intracranial Aneurysm, *Am. J. Neuroradiol.* 24 (2003) 559-566.

[56] G. R. Stuhne and D. A. Steinman, Finite-Element Modeling of the Hemodynamics of Stented Aneurysms, *ASME J. Biomech. Eng.* 126 (2004) 382-387.

[57] J. R. Womersley, Method for the calculation of velocity, rate of flow and viscous drag in arteries when the pressure gradient is known, *J. Physiol.* 127 (1955) 553-563.

[58] M. H. Friedman, V. O'Brien and L. W. Ehrlich, Calculations of pulsatile flow through a branch: implication for the hemodynamics of atherogenesis, *Circ. Res.* 36 (1975) 277-285.

[59] R. Mehrotra, G. Jayaraman and N. Padmanabhan, Pulsatile blood flow in a stenosed artery - a theoretical model, *Med. Biol. Eng. Comput.* 23 (1985) 55-62.

[60] D. M. Wang and J. M. Tarbell, Numerical analysis of flow in an elastic tube (artery): steady streaming effects, *J. Fluid Mech.* 239 (1992) 341-358.

[61] G. R. Zendehbudi and M. S. Moayeri, Comparison of physiological and simple pulsatile flows through stenosed arteries, *J. Biomech.* 32 (1999) 959-965.

[62] D. Zeng, Z. Ding, M. H. Friedman and C. R. Ethier, Effects of cardiac motion on right coronary artery hemodynamics, *Ann. Biomed. Eng.* 31 (2003) 420-429.

[63] S. S. Varghese and S. H. Frankel, Numerical modeling of pulsatile turbulent flow in stenotic vessels, *ASME J. Biomech. Eng.* 125 (2003) 445-460.

[64] I. Marshall, S. Zhao, P. Papathanasopoulou, P. Hoskins and X. Y. Xu, MRI and CFD studies of pulsatile flow in healthy and stenosed carotid bifurcation models, *J. Biomech.* 37 (2004) 679-687.

[65] Y. I. Cho and K. R. Kensey, Effects of the non-Newtonian viscosity of blood on flows in a diseased arterial vessel. Part I: steady flows, *Biorheology.* 28 (1991) 241-262.

[66] Z. Luo and W. J. Yang, A computer simulation of the non-Newtonian blood flow at the aortic bifurcation, *J. Biomech.* 26 (1993) 37-49.

[67] C. Tu and M. Deville, Pulsatile flow of non-Newtonian fluids through arterial stenoses, *J. Biomech.* 28 (1996) 899-908.

[68] F. J. H. Gijsen, E. Allanic, F. N. van de Vosse and J. D. Janssen, The influence of the non-Newtonian properties of blood on the flow in large arteries: unsteady flow in a 90° curved tube, *J. Biomech.* 32 (1999) 705-713.

[69] F. J. H. Gijsen, F. N. van de Vosse and J. D. Janssen, The influence of the non-Newtonian properties of blood on the flow in large arteries: steady flow in a carotid bifurcation model, *J. Biomech.* 32, (1999) 601-608.

[70] K. Rohlf and G. Tenti, The role of the womersley number in pulsatile blood flow - a theoretical study of the casson model, *J. Biomech.* 34 (2001) 141-148.

[71] B. M. Johnston, P. R. Johnston, S. Corney and D. Kilpatrick, Non-Newtonian blood flow in human right coronary arteries: steady state simulations, *J. Biomech.* 37 (2004) 709-720.

[72] S. Amornsamankul, B. Wiwatanapataphee, Y. H. Wu and Y. Lenbury, Effect of Non-Newtonian behaviour of blood on pulsatile flows in stenotic arteries, *Int. J. Biomed. Sci.* 1 (2006) 42-46.

[73] K. Zygourakis, Quantification and regulation of cell migration, *Tissue Eng.* 2 (1) (1996) 1-26.

[74] L. B. Smilenov, A. Mikhailov, R. J. Pelham Jr., E. E. Marcantonio and G. G. Gundersen, Focal adhesion motility revealed in stationary fibroblasts, *Science.* 286 (1999) 1172-1174.

[75] M. J. Kim and K. S. Breuer, Enhanced diffusion due to motile bacteria, *Phys. Fluids.* 16 (9) (2004) 78-81.

[76] N. Darnton, L. Turner, K. Breuer and H. C. Berg, Moving Fluid with Bacterial Carpets, *Biophys. J.* 86 (2004) 1863-1870.

[77] R. M. Ford, B. R. Phillips, J. A. Quinn and D. A. Lauffenburger, Measurement of bacterial random motility and chemotaxis coefficients: I. stopped-flow diffusion chamber assay, *Biotechnol. Bioeng.* 37 (1991) 647-660.

[78] P. D. Frymier, R. M. Ford, H. C. Berg and P. T. Cummings, Three-dimensional tracking of motile bacteria near a solid planar surface, *Proc. Natl. Acad. Sci.* 92 (1995) 6195-6199.

[79] M. A.-S. Vigeant, R. M. Ford, M. Wagner and L. K. Tamm, Reversible and irreversible adhesion of motile escherichia coli cells analyzed by total internal reflection aqueous fluorescence microscopy, *Appl. Environ. Microbiol.* 68 (6) (2002) 2794-2801.

[80] R. L. Satcher Jr., S. R. Bussolari, M. A. Gimbrone Jr. and C. F. Dewey Jr., The Distribution of fluid forces on model arterial endothelium using computational fluid dynamics, *J. Biomech. Eng.* 114 (3) (1992) 309-316.

[81] K. A. Barbee, T. Mundel, R. Lal and P. F. Davies, Subcellular distribution of shear stress at the aurface of flow-aligned and nonaligned endothelial monolayers, *Am. J. Physiol.* 268 (1995) 1765-1772.

[82] P. F. Davies, A. Remuzzi, E. J. Gordon, C. F. Dewey Jr. and M. A. Gimbrone Jr., Turbulent fluid shear stress induces vascular endothelial cell turnover in vitro, *Proc. Natl. Acad. Sci.* 83 (1986) 2114-2117.

[83] J. A. Frangos, L. V. McIntire and S. G. Eskin, Shear stress induced stimulation of mammalian cell metabolism, *Biotech. Bioeng.* 32 (1988) 1053-1060.

[84] N. Kataoka, S. Ujita and M. Sato, Effect of flow direction on the morphological responses of cultured bovine aortic endothelial cells, *Med. Biol. Eng. Comput.* 36 (1998) 122-128.

[85] H. Jeon, Y. Lee, S. Jin, S Koo, C-S. Lee and J. Y. Yoo, Quantitative analysis of single bacterial chemotaxis using a hydrodynamics focusing channel, *Trans. KSME B.* 31 (3) (2007) 209-216.

[86] T. Yamaguchi, Y. Yamamoto and H. Liu, Computational mechanical model studies on the spontaneous emergent morphogenesis of the

cultured endothelial cells, *J. Biomech.* 33 (2000) 115-126.

[87] R. Mesibov and J. Adler, Chemotaxis toward Amino Acids in Escherichia Coli, *J. Bacteriol.* 112 (1) (1972) 315-326.

[88] J. Diao, L. Young, S. Kim, E. A. Fogarty, S. M. Heilman, P. Zhou, M. L. Shuler, M. Wu and M. P. DeLisa, A three-channel microfluidic device for generating static linear gradients and its application to the quantitative analysis of bacterial chemotaxis, *Lab Chip.* 6 (2006) 381-388.

[89] N. L. Jeon, H. Baskaran, S. K. W. Dertinger, G. M. Whitesides, L. V. D. Water and M. Toner, Neutrophil chemotaxis in linear and complex gradients of interleukin-8 formed in a microfabricated device, *Nat. Biotech.* 20 (2002) 826-830.

[90] H. Mao, P. S. Cremer and M. D. Manson, A sensitive, versatile microfluidic assay for bacterial chemotaxis, *Proc. Natl. Acad. Sci.* 100 (9) (2003) 5449-5454.

[91] Y. Lee, S. Jin, S. Koo and J. Y. Yoo, On the dynamic characteristics of cell contact by analyzing TIRF Images, *Trans. KSME A.* 31 (3) (2007) 380-387.

[92] Y. Lee, S. Koo and J. Y. Yoo, Cell-based drug-screening method using total internal reflection microscopy, *Proc. MNC2007. ICMN. ASME.* (2007).

[93] P. Friedl and K. Wolf, Tumour-cell invasion and migration: diversity and escape mechanisms, *Nat. Rev.* 3 (2003) 362-374.

[94] K. Murata, M. Kameyama, F. Fukui, H. Ohigashi, M. Hiratsuka, Y. Sasaki, T. Kabuto, M. Mukai, T. Mammoto, H. Akedo, O. Ishikawa and S. Imaoka, Phosphodiesterase type III inhibitor, cilostazol, inhibits colon cancer cell motility, *Clin. Exp. Metastasis.* (1999) 525-530.